In vitro response and gene expression of human retinal Müller cells treated with different anti-VEGF drugs

Javier Cáceres-del-Carpio[a,1,2,#]; M. Tarek Moustafa[a, 3, #]; Jaime Toledo-Corral[a]; Mohamed A. Hamid[a,3]; Shari R. Atilano[a]; Kevin Schneider[a]; Paula S. Fukuhara[a]; Rodrigo Donato Costa[a,4] J. Lucas Norman[a]; Deepika Malik[a,5]; Marilyn Chwa[a]; David S. Boyer[b]; G. Astrid Limb[c]; M. Cristina Kenney[a,d*]; Baruch D. Kuppermann[a,e]

[a] Gavin Herbert Eye Institute, University of California, Irvine, CA, USA; [b] Retina-Vitreous Associates Medical Group, Los Angeles, CA, USA; [c] Division of Ocular Biology and Therapeutics, UCL Institute of Ophthalmology, London, UK; [d] Department of Pathology and Laboratory Medicine, University of California, Irvine, CA, USA; [e] Department of Biomedical Engineering, University of California, Irvine, USA

*Corresponding author. Ophthalmology, 843 Heath Science Road, Hewitt Hall, Room 2018, Gavin Herbert Eye Institute, University of California, Irvine, Irvine, CA, 92697, USA

# These authors contributed equally to this article.

1. Facultad de Medicina Humana Manuel Huaman Guerrero – Universidad Ricardo Palma, Lima, Peru.
2. Ophthalmology Service, Hospital Nacional Edgardo Rebagliati Martins – EsSalud, Lima, Peru.
3. Ophthalmology Department, Minia University, Egypt.
4. Instituto Donato Oftalmologia, Poços de Caldas, MG, Brazil.
5. Laurel Eye Clinic, Brookville, Pennsylvania, USA.

1. Introduction

In the past decade, anti-vascular endothelial growth factor (VEGF) therapy has become more popular and the standard of care for several retinal diseases including exudative age-related macular degeneration (AMD) (Brown et al., 2006; Martin et al., 2012; Rosenfeld et al., 2006; Tufail et al., 2010), diabetic macular edema (DME) (Brown et al., 2013; Do et al., 2012; Do et al., 2013; TDRCR, 2015), and macular edema (ME) due to retinal vein occlusion (RVO) (Brown et al., 2010, 2013; Campochiaro et al., 2010; Wu et al., 2008).

Ranibizumab (Lucentis®, Genentech, South San Francisco, CA) is a humanized, recombinant, monoclonal antibody fragment. Intended for intraocular use, a 0.5mg/0.05 ml dose is approved by the Food and Drug Administration (FDA) for exudative AMD and ME due to RVO; a 0.3mg/0.05 ml dose is approved by the FDA for DME, and diabetic retinopathy (DR). Bevacizumab (Avastin®, Genentech, South San Francisco, CA) is a humanized monoclonal human immunoglobulin gamma 1 (IgG1) antibody that selectively binds to circulating VEGF and inhibits its binding to cell surface receptors. A 1.25mg/0.05 ml concentration is used off-label in the United States and is commonly used worldwide for exudative AMD, DME and RVO. Aflibercept (Eylea®, Regeneron Pharmaceuticals, Tarrytown, NY) is a recombinant protein receptor decoy composed of two VEGF receptors 1 and 2 fused with the Fc region of human IgG1. Compared to the former two anti-VEGF drugs, it has a higher binding affinity for VEGF and it also binds to VEGF-B and Placental growth factor (PGF). A concentration of 2.0mg/0.05 ml is approved by the FDA for wet AMD, DME, ME due to RVO, and DR in patients with DME.

Ziv-aflibercept (Zaltrap®, Sanofi Aventis, Bridgewater, NJ and Regeneron Pharmaceuticals, Tarrytown, NY), also known as VEGF Trap-oncologic, contains 25 mg/ml ziv-aflibercept as well as higher sucrose concentrations than aflibercept (Eylea), which results in higher osmolality (Bayer, 2014; Group, 2012). Ziv-aflibercept is approved by the FDA for treatment of resistant or progressing metastatic colorectal cancer. However, Mansour et al., 2015, 2017a, 2017b; de Oliveira Dias et al. (de Oliveira Dias et al., 2015; de Oliveira Dias et al., 2017; de Oliveira Dias et al., 2016); and Chhablani et al., (Chhablani, 2015; Chhablani et al., 2017), among other authors, have published several reports finding good outcomes and no apparent safety issues in a series of patients treated with intravitreal ziv-aflibercept.

Previous studies have shown that anti-VEGF drugs in clinically significant doses do not affect cell viability *in vitro* in a human retinal pigment epithelium (RPE) cell line (ARPE-19) (Luthra et al., 2006; Malik et al., 2014b). Nonetheless, subtle cytotoxic changes in RPE cells, such as a decrease in mitochondrial membrane potential, could be observed even at clinical doses for some anti-VEGF drugs (Malik et al., 2014b). Numerous publications have described *in vitro* differential responses to the different anti-VEGF drugs in various retinal cells (Deissler et al., 2012; Klettner et al., 2010; Schnichels et al., 2013).

Müller cells are the predominant glial cells in the retina and provide structural and metabolic support to retinal neurons. Several studies have described numerous functions of Müller cells, including regulation of cellular homeostasis and pH, modulation of neurotransmitter recycling, contribution to the blood-retinal barrier by surrounding retinal capillaries with glial processes (Limb et al., 2002; Reichenbach and Bringmann, 2013), acting as light collectors by directing light to photoreceptors (Franze et al., 2007; Reichenbach and Bringmann, 2013), and secretion and regulation of VEGF and pigment epithelium derived factor (PEDF) (García and Vecino, 2003; Limb et al., 2002; Reichenbach and Bringmann, 2013). Müller cells have also been associated with retinal neuroprotection, wound healing and regeneration (García and Vecino, 2003).

The purpose of this study was to evaluate the *in vitro* response and differences in gene expression of human retinal Müller cells treated with different concentrations of ranibizumab, bevacizumab, aflibercept or ziv-aflibercept. Assays for cell viability, metabolic activity, mitochondrial membrane potential (ΔΨm), reactive oxygen species (ROS) and apoptosis were used to evaluate responses to the anti-VEGF drugs. In addition, differences in the expression levels for angiogenesis-related, pro-apoptotic, inflammation and oxidative stress genes were assessed.

2. Methods

2.1. Cell culture

The immortalized human retinal Müller cell line MIO-M1 was obtained from the Department of Cell Biology of the University College, London. Cells were cultured in Dulbecco's Modified Eagle's Medium (DMEM) with 4.5 g/L glucose, glutaGRO (Corning Cellgro, Manassas, VA), and 10% fetal bovine serum (FBS) as reported previously (Hollborn

et al., 2011; Limb et al., 2002; Ramírez et al., 2016). It should be noted that the glucose levels in both control and treated media are higher than that of healthy individuals (normal glucose levels in the body are 70–130 mg/dL) and may have some influence on the viability of the cultured cells as well as the expression of different genes. However, the MIO-M1 cell line requires higher glucose levels for healthy culture conditions and some reports in the literature showed that these high glucose levels in the culture media did not affect gene expression levels (Matsuzaki et al., 2014). In this study, MIO-M1 cells were plated in either 6-well, 24-well or 96-well plates for 24 h before treatment and kept under normal culture conditions of 37 °C and 5% carbon dioxide.

2.2. Markers for MIO-M1 cell line

The morphology of cultured MIO-M1 cells was evaluated by phase contrast microscopy and compared to the original study describing the cell line (Limb et al., 2002). Quantitative real-time-PCR (qRT-PCR) was used to measure expression levels of genes known to be markers for human retinal Müller cells and compared to ARPE-19 cell markers.

Tissue culture: MIO-M1 cells were cultured as described above. The ARPE-19 cells were obtained from ATTCC (Manassas, VA) and cultured in DMEM mixture 1:1 Ham's F-12 medium (Corning–Cellgro, Mediatech, Manassas, VA), with 10% FBS, penicillin F 100 U/ml, streptomycin sulfate 0.1% mg/mL, gentamicin 10 mg/mL, and amphotericin B 2.5 mg/mL. Briefly, MIO-M1 cells and ARPE-19 cells were plated in 6-well plates and cultured for 24 h.

RNA extraction and cDNA synthesis: RNA was isolated using the RNeasy Mini-Extraction kit (Qiagen, Inc., Valencia, CA). cDNA was synthesized from 100 ng of each RNA sample using the SuperScript-VILO cDNA Synthesis Kit (Invitrogen - Life Technologies, Eugene, OR).

Gene expression analyses: qRT-PCR (QuantiTect Primer Assay, Qiagen, Inc., Valencia, CA) was performed using primers for actin, alpha 2, smooth muscle, aorta (*ACTA2*, Gene ID 59, NM_00114945) and Glial Fibrillary Acidic Protein (*GFAP*, Gene ID 2670, NM_002055) (Limb et al., 2002). Low levels of retinaldehyde binding protein 1 (*CRALBP,* Gene ID 6017, NM_000326) can also be found in Müller cells (Burke, 2008; Dunn et al., 1996; Limb et al., 2002; Reichenbach and Bringmann, 2013).

For comparison, the levels for three known markers for RPE cells, *BEST1* (Gene ID 7439, NM_004183) (Burke, 2008), *CRALBP* (Gene ID 6017, NM_000326) (Burke, 2008; Dunn et al., 1996) and *KRT18* (Gene ID 3875, NM_000224) (Burke, 2008) (a marker for RPE differentiation) were measured. Each of the marker genes were compared to the housekeeper gene Hydroxymethylbilane Synthase (HMBS, Gene ID 3145, NM_000190, NM_001024382, NM_001258208, NM_001258209). Subsequently, fold differences of the MIO-M1 cells and ARPE-19 cells were calculated. The samples were run in triplicate and the experiment repeated twice.

qRT-PCR was performed using Power SYBR green master mix on a StepOnePlus Q-PCR system (Applied Biosystems - Life Technologies, Eugene, OR). ΔCt values for each marker gene of interest were calculated through normalization to the internal control HMBS. ΔΔCt values were obtained through comparison of MIO-M1 and ARPE-19 ΔCt values. Folds were calculated with the formula $2^{\Delta\Delta Ct}$.

The ARPE-19 cells were assigned a value of 1 for each of the markers (Fig. 1A). In the MIO-M1 cells, the genes expression levels of *ACTA2* (3.4-fold, p = 0.0003) and *GFAP* (21.6-fold, p = 0.01) were significantly higher than transcription levels seen in human ARPE-19 cells (1.0-fold). In contrast, the MIO-M1 cells had very low levels for the three known markers for RPE cells, *BEST1* (0.011-fold, p = 0.0001), *CRALBP* (0.16-fold, p = 0.0007) and *KRT18* (0.016-fold, p = 0.0001) relative to the ARPE-19 cells (1.0-fold).

<u>Phase contrast microscopy:</u> MIO-M1 cells were plated in 96-well plates and placed in an IncuCyte instrument (Essen Bioscience, Inc, Ann Arbor, MI) for 72 h. Images were captured at 24 and 72 h. Fig. 1B shows subconfluent monolayer of MIO-M1 cells displaying bipolar morphology, elongated cytoplasmic projections and a granular intracellular profile, similar to that described by Limb and coworkers (Limb et al., 2002). Fig. 1C shows that confluent MIO-M1 cells maintain their spindle shape and granular appearance.

Some MIO-M1 cultures were treated with anti-VEGF drugs for 24 h and the IncuCyte® Caspase-3/7 Green Apoptosis Assay Reagent probe (Cat. No. 4440, DNA intercalating dye) was added to measure the levels of apoptosis. This probe is non-perturbing to cell growth and morphology of *in vitro* systems. When apoptosis occurs, this inert probe crosses the cell membrane, is cleaved by activated Caspase 3/7 and becomes fluorescent. The excitation

wavelength is 500 nm and the emission wavelength is 530 nm. All analysis was done utilizing the IncuCyte S3 2019A software (Essen Bioscience, Inc. Ann Arbor, MD). Caspase-3 levels were normalized to nuclear count as measured by Nuclight Live Cell imaging Reagent (Cat. No. 4625).

2.3. Treatments

Cells were treated for 24 h with either ranibizumab, bevacizumab, aflibercept or ziv-aflibercept in 1x and 2x concentrations. The 1x clinical dose was defined as 0.05 ml injected into 4 ml vitreous, which is equivalent to 0.5 mg ranibizumab, 1.25 mg bevacizumab and 2 mg aflibercept. For ziv-aflibercept, for which the commercially available concentration is 25 mg/ml, 1x was the clinical equivalent dose to aflibercept (2.0 mg in 0.05 ml) injected in 4 ml of vitreous. Under tissue culture conditions, the 1x and 2x drug concentrations were equivalent to the clinical doses described above.

2.4. Cytotoxicity assays

2.4.1. Cell viability assay (Trypan blue dye exclusion assay)

MIO-M1 cells were plated in 6-well plates with a concentration of 0.5×10^6 cells per well for 24 h, and treated for an additional 24 h with the four drugs at the different concentrations. Cells were harvested and cell viability (CV) was assessed by trypan blue dye exclusion with an automated ViCell cell viability analyzer (Beckman Coulter Inc., Fullerton, CA). This assay is based on the principle that cells with intact membranes can exclude the trypan blue dye while dead cells are permeable and uptake the dye. Results were normalized to untreated 100%.

2.4.2. Cellular metabolic activity (MTT assay)

Cells were plated in 96-well plates at 20×10^3 cells per well and treated accordingly as described previously. As per the manufacturer's protocol, 10 µl of tetrazolium MTT dye (3-(4,5-dimethylthiazol-2-yl)-2,5-diphenyltetrazolium bromide; Biotium, Hayward, CA) were added to each well; after 1.5 h incubation at 37 °C, 200 µl of dimethyl sulfoxide (DMSO) were added to each well. Absorbance signal at 570 nm and background absorbance at 630 nm were measured using a BioTek ELx808 absorbance plate reader (BioTek, Winooski, VT). Absorbance ratios were normalized to untreated 100%. The MTT assay, which assesses

the metabolism of yellow tetrazolium MTT salt into purple formazan crystal by active cells, is quantified by measuring the absorbance and is proportional to the number of viable cells (Mosmann, 1983).

2.4.3. Mitochondrial membrane potential (ΔΨm)

1×10^5 cells per well were plated in 24-well plates and treated with anti-VEGF drugs as described previously. The JC-1 detection kit (Biotium Inc., Hayward, CA) was used to assess the ΔΨm. The JC-1 dye (5,5',6,6'-tetrachloro-1,1',3,3'-tetraethyl-benzimidazolyl-carbocyanine-iodide) is a cationic dye that accumulates in the mitochondrial membranes of healthy cells resulting in red fluorescence. Stressed or damaged cells show reduced ΔΨm and accumulate the dye in the cytosol instead of in the mitochondria, resulting in green fluorescence. To obtain the changes in ΔΨm, the ratio of red to green fluorescence was calculated. Cells were exposed to a 1:100 solution of the stock JC-1 dye in phenol-red free medium and incubated in 37 °C for 15 min. A Biotek Synergy HT plate reader (Biotek, Winooski, VT) was used to measure the fluorescent signals, set to detect green (excitation (EX) 485 nm, emission (EM) 535 nm) and red (EX 550 nm, EM 600 nm) emissions; and red to green ratios were calculated. Results were normalized to untreated 100%.

2.4.4. Reactive oxygen species (ROS) production

Cells were plated in 24-well plates and treated as described previously. ROS production was assessed using the fluorescent dye 2',7'-dichlorodihydrofluorescein diacetate (H2DCF-DA; Molecular Probes–Life Technologies, Eugene, OR). This assay detects hydrogen peroxide, hydroxyl radicals, and peroxynitrite anions. Cells were exposed to 10 μM of H2DCF-DA in PBS and incubated for 30 min at 37 °C. The fluorescent signal was measured using the Biotek Synergy HT plate reader (Biotek, Winooski, VT) with EX filter in 490 nm and EM filter in 520 nm. Results were normalized to untreated 100%.

2.4.5. YO-PRO-1 apoptosis assay

Cells were plated in 24-well plates and treated accordingly. YO-PRO-1 iodide (Molecular Probes-Life Technologies, Eugene, OR) is a nucleic acid dye that enters cells in early stages of apoptosis without interfering in cell viability (Glisic-Milosavljevic et al., 2005; Idziorek et al., 1995). Apoptotic cells show green fluorescence. Cells were exposed to 1 μM of YO-PRO-1

dye in phenol-red free medium and incubated for 20 min over ice. A Biotek synergy HT plate reader (Biotek, Winooski, VT) was used to measure fluorescence with EX 491 nm and EM 509 nm. Results were normalized to untreated 100%.

2.5. Gene expression

Cells were plated in 6-well plates and treated with the anti-VEGF drugs as described previously. RNA was isolated using the RNeasy Mini-Extraction kit. cDNA was synthesized from 100 ng of each RNA sample using the SuperScript-VILO cDNA Synthesis Kit (Invitrogen-Life Technologies, Eugene, OR). Quantitative polymerase chain reaction (qRT-PCR) was performed using primers (QuantiTect Primer Assay, Qiagen, Inc., Valencia, CA) for the following genes (Table 1). The angiogenesis-related genes included vascular endothelial growth factor A (*VEGFA*), placental growth factor (*PGF* or *PlGF*) and hypoxia inducible factor 1 alpha (*HIF1A*); key regulatory genes responsible for neovascularization in many disease processes. Apoptosis is a common feature of the retinal degeneration occurring in AMD, and two representative pro-apoptotic genes, B-cell lymphoma 2 like 13 (*BCL2L13*) and BCL2-associated X protein (*BAX*), were analyzed in our cultures. The genes representing the inflammation pathway were interleukin 1 beta (*IL1β*) and interleukin 18 (*IL18*), which are increased with aging, expressed after Caspase-1 activation and accumulate in chronic retinal degenerations, including AMD (Campbell et al., 2014; Franceschi and Campisi, 2014; Goldberg and Dixit, 2015). The anti-oxidative enzyme genes measured were glutathione peroxidase 3 (*GPX3*) and superoxide dismutase 2 (*SOD2*), both of which are important for removal of hydrogen peroxide and superoxide from retinal cells, respectively. Knockdown of SOD2 within the RPE cells of a mouse results in a mouse model with key features of AMD (Biswal et al., 2016).

qRT-PCR were performed using Power SYBR green master mix on a StepOnePlus Q-PCR system. Housekeeper genes with comparable amplification efficiencies were chosen: Aminolevulinic Acid Synthase variant 1 (*ALAS1* for *GPX*, *PGF*, *HIF1α* and *IL1β* genes), hypoxanthine-guanine phosphoribosyl transferase (*HPRT1* for *SOD2*, *VEGFA*, *IL18* and *BAX* genes) and hydroxymethylbilane synthase (*HMBS* for *BCL2L13* gene). For gene expression analysis, qRT-PCR was run in triplicate; ΔΔCt values were obtained and folds were calculated with the formula $2^{\Delta\Delta Ct}$. The gene expression

levels of untreated controls were assigned a value of 1. Fold values > 1 indicate gene upregulation and fold values < 1 indicate gene downregulation.

2.6. Statistical analyses

Data were analyzed with unpaired *t*-test using the GraphPad Prism version 5.00 for Windows (GraphPad Software, San Diego, CA). Error bars in the graphs represent standard error of mean (SEM). For CV, MTT, ΔΨm, ROS and apoptosis assays: experiments were run in quadruplicate and repeated three times; all the results were normalized to the untreated control as 100%. Values of $p < 0.05$ (*) statistically significant; $p < 0.01$ (**) very significant; $p < 0.001$ (***) extremely significant.

3. Results

3.1. Dye exclusion cell viability (CV)

Human Müller cells exposed to ranibizumab, bevacizumab, aflibercept or ziv-aflibercept showed no significant difference in mean percentage CV (CV%) in any of the drugs and any of the concentrations used compared to untreated cultures. Ranibizumab showed CV% of 95.84 ± 0.50, 95.50 ± 0.50 and 95.20 ± 0.39; and bevacizumab showed 95.51 ± 0.31, 95.06 ± 0.48 and 96.06 ± 0.39 of CV% for untreated, 1x and 2x, respectively (Fig. 2A and B). Aflibercept showed 96.23 ± 0.57 for untreated, 95.43 ± 0.57 for 1x and 95.80 ± 0.37 for 2x dose (Fig. 2C). CV% of 95.23 ± 0.68, 96.18 ± 0.65 and 94.60 ± 0.52 were observed for ziv-aflibercept untreated, 1x and 2x respectively (Fig. 2D).

3.2. MTT assay

Retinal Müller cells exposed to all the drugs in both concentrations, showed significantly lower relative cell growth (lower tetrazolium MTT salt metabolism) when compared to untreated 100%. Ranibizumab showed 85.65 ± 1.15 and 88.17 ± 1.94, with $p < 0.0001$ and $p = 0.0004$ for 1x and 2x, respectively (Fig. 3A). Bevacizumab showed 83.57 ± 1.69 ($p < 0.0001$) and 87.92 ± 2.48 ($p = 0.0012$) for 1x and 2x doses, respectively (Fig. 3B). Aflibercept presented 81.72 ± 1.51 ($p < 0.0001$) for 1x, and 85.44 ± 2.63 ($p = 0.0002$) for 2x doses (Fig. 3C). Ziv-aflibercept showed 84.89 ± 1.47 for 1x and 81.65 ± 1.66 for 2x, with $p < 0.0001$ for both concentrations (Fig. 3D).

3.3. Mitochondrial membrane potential (ΔΨm)

MIO-M1 cells exposed to ranibizumab showed no significant difference in mitochondrial membrane potentials for 1x dose (99.33 ± 2.31) and 2x dose (97.34 ± 2.31) compared to untreated cultures normalized to 100% (Fig. 4A). Cells exposed to bevacizumab (1x dose) (93.87 ± 3.72) showed no significant difference in ΔΨm compared to untreated. However, the 2x dose (85.74 ± 4.49) was significantly lower than untreated controls (p = 0.03) (Fig. 4B). For aflibercept, the 1x dose showed mitochondrial membrane potential of 85.28 ± 2.87 (p = 0.0008) and the 2x dose demonstrated 85.02 ± 3.80 (p = 0.0031), respectively, when compared to untreated (Fig. 4C). Ziv-aflibercept showed a decrease in ΔΨm for 1x dose 85.39 ± 3.47 (p = 0.0016) and 2x with 86.01 ± 4.62, (p = 0.0116), respectively when compared to untreated (Fig. 4D).

3.4. ROS

Retinal Müller cells exposed to ranibizumab showed increased levels of ROS at the 1x (136.90 ± 4.67) and 2x (139.83 ± 6.53) doses with p < 0.0001 for both when compared to untreated (Fig. 5A). Higher ROS levels were also found for bevacizumab at the 1x (124.13 ± 5.47, p = 0.0017) and 2x (133.92 ± 8.10, p = 0.0011) doses as compared to untreated (Fig. 5B). Aflibercept at the 1x dose showed ROS levels of 129.62 ± 3.08 whereas the 2x dose showed 130.27 ± 4.58, with p < 0.001 for both compared to untreated (Fig. 5C). Higher levels for ROS were also found for Ziv-aflibercept at the 1x (140.27 ± 9.92, p = 0.0001) and 2x (144.28 ± 12.02, p = 0.0004) doses when compared to untreated (Fig. 5D).

3.5. YO-PRO-1 apoptosis

MIO-M1 cells showed higher levels of early apoptosis compared to untreated cultures when exposed to all the drugs in both concentrations. Ranibizumab 1x dose showed 133.48 ± 8.35 (p = 0.0107), ranibizumab 2x dose 141.35 ± 7.40 (p = 0.0039), bevacizumab 1x dose 133.26 ± 7.95 (p = 0.0037), bevacizumab 2x dose 140.21 ± 7.68 (p = 0.0005), aflibercept 1x dose 169.17 ± 12.23 (p = 0.0001), aflibercept 2x dose 179.00 ± 11.23 (p < 0.0001), ziv-aflibercept 1x dose 154.72 ± 13.19 (p = 0.0062), and ziv-aflibercept 2x dose 171.16 ± 17.36 (p = 0.0039) when compared to untreated cultures normalized to 100% (Fig. 6A–D). During the IncuCyte studies, after a 24-h incubation period with anti-VEGF drugs, the probe for

Caspase-3 levels was added to the cultures and activation levels were measured. There was no significant change in the caspase 3 levels in the anti-VEGF drugs (data not shown).

3.6. Gene expression (Tables 2A–2D)

VEGFA was found to be significantly downregulated in both concentrations of all the drugs studied except in ziv-aflibercept 2x dose. *PGF* was found to be significantly upregulated in bevacizumab 1x and aflibercept 1x and 2x; and significantly downregulated in ziv-aflibercept 1x and 2x. No significant differences were found in the *HIF1A* levels in any of the drugs studied. The *BAX* expression levels were not found to be significantly different except at the 1x bevacizumab and ziv-aflibercept 1x and 2x doses. The *BCL2L13* expression levels were significantly upregulated in 1x ranibizumab, 1x and 2x bevacizumab, 1x and 2x aflibercept, and 1x ziv-aflibercept.

IL1β was significantly upregulated in ranibizumab 1x and 2x and bevacizumab 1x, but was not significantly changed in bevacizumab 2x or any concentration of aflibercept and ziv-aflibercept. *IL18* was significantly upregulated in ranibizumab 1x and ziv-aflibercept 1x and 2x. A significant downregulation for *SOD2* expression was found in both concentrations of all the drugs studied. A significant difference was seen in the upregulation for *GPX3* levels at the 1x and 2x concentrations of ranibizumab, bevacizumab and aflibercept. No significant differences were found for *GPX3* gene in any of the ziv-aflibercept concentrations.

4. Discussion

Anti-VEGF therapy is the mainstay for treatment of many retinal diseases. Previous clinical studies have confirmed its safety and effectiveness in treating AMD (Brown et al., 2006; Martin et al., 2012; Rosenfeld et al., 2006; Tufail et al., 2010), DME (Do et al., 2012; Do et al., 2013; TDRCR, 2015) and RVO (Brown et al., 2010, 2013; Campochiaro et al., 2010; Wu et al., 2008). However, it has the potential to cause increases in the size of geographic atrophy in patients with AMD (Grunwald et al., 2014; Martin et al., 2012) and possibly worsening of macular ischemia in DME (Manousaridis and Talks, 2012).

In this investigation, we tested commercially available anti-VEGF drugs on an immortalized cell line of human retinal Müller cells (MIO-M1). Müller cells have very important functions including maintenance of the blood retinal barrier (Constable and Lawrenson, 2009; Sarthy

and Lam, 1978); secretion and regulation of pigment epithelium derived factor (*PEDF*) and *VEGF* (García and Vecino, 2003; Limb et al., 2002; Reichenbach and Bringmann, 2013) along with neuroprotection during wound healing and regeneration (García and Vecino, 2003). Even after initial improvement of retinal anatomy and visual acuity, some subjects receiving long-term administration of anti-VEGF injections develop geographic atrophy.

In a study by Matsuda et al. in which they exposed the MIO-M1 cell line to bevacizumab 0.25 mg/ml or 0.5 mg/ml and evaluated cell viability (dye exclusion and MTT assays), levels of apoptosis (Caspase-3 gene expression) and autophagy, they found no significant differences in cell viabilities as measured by the trypan blue assay at any bevacizumab concentration or length of exposure which is very similar to our results. When mitochondrial metabolic rates were measured with the MTT assay, they found higher levels at 24 h compared to the 12-h treatment (Matsuda et al., 2017). In contrast, our MIO-M1 cultures, which were cultured for 24 h, showed lowered MTT metabolism for all drugs studied, including bevacizumab.

With respect to apoptosis, Matsuda's group used two bevacizumab concentrations (25 and 50 mg/ml), and reported the increased gene expression of Caspase-3 at the 12-h timepoint, but not at 24 h and suggested that cells may have adapted to the bevacizumab through increased metabolic activity (Matsuda et al., 2017). Romano and co-workers showed TUNEL staining and apoptosis in the retinal ganglion cells of rat eyes 48 h after a single injection of bevacizumab, where the staining significantly increased with multiple injections (Romano et al., 2012). In our study, using 25 mg/ml bevacizumab, we found increased ROS production and early apoptosis as measured by higher YO-PRO-1 levels. The ΔΨm (another marker for early apoptosis) decreased in bevacizumab at the 2x dose, and both concentrations of aflibercept and ziv-aflibercept. However, cell viability, as measured by trypan blue assay, was not decreased at the 24-h time point for any of the anti-VEGF drugs. This was not totally surprising because the trypan blue assay measures viable cells that have intact cell membrane that exclude dyes, indicating when the cells are dead or viable. Caspase-3 levels measured in the MIO-M1 cells after 24 h incubation with anti-VEGF drugs were not significantly elevated compared to the untreated cultures (data not shown). This suggests that the stressed MIO-M1 cells may show signs of early apoptosis (higher YO-PRO-1 and lower ΔΨm) but have not reached the later stages of apoptosis (Caspase-3 activation) so

their cell membranes are still intact and cell viability is normal. Similar results were shown in the ARPE-19 cells, whereby the cell viability was unchanged after a 24-h exposure to the anti-VEGF drugs however, the ΔΨm was decreased (Malik et al., 2014a). Perhaps if we had evaluated the MIO-M1 cultures at later time points and/or used higher concentrations of the anti-VEGF drugs, we may have seen loss of cell viability in addition to the apoptosis changes.

In this investigation, we also studied the effects of these anti-VEGF drugs on cell metabolism, which was first described by Mossman (Mosmann, 1983). The Müller cells showed decreased levels of metabolism/viability at the 1x and 2x doses of the four drugs. These results are consistent with the work on primary porcine RPE cells (Klettner et al., 2010), where bevacizumab and ranibizumab decreased the cellular metabolism/viability. Guo et al. showed no change in the number of viable rat retinal Müller glial cells (RMGCs) after 72 h of treatment with bevacizumab as determined using both the trypan blue dye exclusion and MTT colorimetric assays (Guo et al., 2010). A study by Spitzer et al. (2007), initially tested the effects of bevacizumab on different ocular cells (human RPE, rat retinal ganglion cells (RGC5), and pig choroidal endothelial cells (CEC), and discovered decreased incorporation of 5'-bromo-2'-deoxyuridine (BrdU) cell after 2 days.

In our gene expression studies, we found decreased expression levels of *VEGFA* in all drug concentrations expect 2x ziv-aflibercept. *PGF* levels were not changed in ranibizumab treated cells but had increased expression in the bevacizumab and aflibercept treated MIO-M1 cells. In contrast, the *PGF* levels were downregulated in ziv-aflibercept treated cultures. There was no change in the *HIF1A* gene expression level in any of the anti-VEGF treated cultures. Our results are consistent with the clinical studies by Zehetner et al., who measured the PGF and VEGFA levels in blood samples of patients with wet AMD treated with intravitreal aflibercept, ranibizumab or bevacizumab and demonstrated that the aflibercepttreated patients had decreased plasma VEGFA levels and increased PGF levels (Zehetner et al., 2015). In contrast, the ranibizumab and bevacizumab treated subjects showed decreased levels of both VEGFA and PGF.

The MIO-M1 cells responded differently when treated with ziv-aflibercept compared to treatments with the other anti-VEGF drugs. For example, after treatment with 1x and 2x ziv-aflibercept, the PGF levels decreased while the levels increased with aflibercept and

bevacizumab treatment or remained unchanged with ranibizumab treatment. Both aflibercept and ziv-aflibercept have the same active drug, which is a soluble decor receptor that binds to VEGFA, VEGFB and PLGF with greater affinity than their natural receptors, thereby inhibiting the formation of new blood vessels. However, aflibercept was formulated for intraocular use, while ziv-aflibercept was formulated for intravenous application in cancer patients (Singh et al., 2017). The osmolarity of ziv-aflibercept is between 815 and 820mOsm, which can be tolerated when introduced into the blood stream, while aflibercept's osmolarity is between 250 and 260 mOsm. This level could be less toxic when placed into the relatively small volume of the vitreous chamber. In cultures of ARPE-19 cells treated with anti-VEGF drugs, the osmolality of 10x ziv-aflibercept was 418 mOsm while aflibercept was 317 mOsm (Malik et al., 2014b). Hollborn et al. reported that RPE cells grown in hyperosmotic media showed altered gene transcription of VEGF, as well as aquaporin water channel genes (Hollborn et al., 2011). It may be that the higher mOsm environmental changes the effective binding capacity of ziv-aflibercept resulting in a different regulation of PGF and VEGFA gene expressions compared to the aflibercept drug.

There were also consistent differences in gene expression levels of *PGF, BAX, BCL2L13, IL18* and *GPX3* observed in the aflibercept versus ziv-aflibercept treated cultures. Again, this may be due to the pharmacological alterations of the ziv-aflibercept formulation of higher sucrose (Group, 2012) and osmolality values compared to aflibercept (Bayer, 2014; Group, 2012; Malik et al., 2014b). The parent pharmaceutical company has consistently warned that the ziv-aflibercept formulation is not compatible with intraocular use. Our *in vitro* findings support that the cellular responses to aflibercept and ziv-aflibercept treatments are different and therefore may not be considered to be inter-changeable drugs.

The overexpression levels of the *BCL2L13*, a pro-apoptotic gene, in cultures treated with anti-VEGF drugs are consistent with our finding of increased apoptosis. In ranibizumab-treated MIO-M1 cells, the pro-inflammatory genes (*IL1β* and *IL18*) were also overexpressed compared to untreated cells. This finding coincides with Golan and coworkers who demonstrated that in hypoxic conditions, the ranibizumab or bevacizumab-treated human ARPE-19 and umbilical vein (EA.hy926) also showed altered expression of pro-inflammatory genes (Golan et al., 2014).

A limitation to our study was the use of our transformed cell lines (MIO-M1) to address retinal biology due to the varying nature of these cultures from the non-transformed retinal cells. Using array analyses, the gene expression between transformed and native cell lines can be different based on external factors and stimulation (Tian et al., 2005). Therefore, the results obtained from our *in vitro* cell culture studies are valuable, but additional studies using primary Müller cells isolated from chick (Rios et al., 2019), mouse (Ozawa et al., 2019) or rat retinas (Pereiro et al., 2018) are required and will be the focus of future studies.

5. Conclusions

In our MIO-M1 cultures, the anti-VEGF drugs caused decreased metabolism, viability and mitochondrial membrane potential, along with increased ROS and apoptosis levels. The anti-VEGF treated cultures demonstrated altered gene expression levels in antioxidant, pro-apoptotic and pro-inflammatory pathways. These findings indicate that in MIO-M1 cells *in vitro*, the anti-VEGF drugs can mediate expression of non-angiogenesis pathways genes and may contribute to the cytotoxicity associated with chronic anti-VEGF injections.

Financial disclosure

All authors have no financial interest to disclose related to this work except the last author, Baruch D. Kuppermann who is a consultant to Alcon, Alimera, Allegro, Allergan, Catalyst, Cell Care, Cell-Cure, Dose, Eyedaptic, Genentech, Glaukos, GSK, J-Cyte, Novartis, Ophthotech, Re-Vana, Regeneron, Santen, ThromboGenics. M. Cristina Kenney; Discovery Eye Foundation is a 501(c)3 that has supported her mitochondrial research. She serves as a Board Member for DEF. The terms of this arrangement have been reviewed and approved

References

Bayer, 2014. Eylea™/VEGF Trap-Onc: Ophthalmic vs Systemic Formulations. Bayer

HealthCare.

Biswal, M.R., Ildefonso, C.J., Mao, H., Seo, S.J., Wang, Z., Li, H., Le, Y.Z., Lewin, A.S.,

2016. Conditional induction of oxidative stress in RPE: a mouse model of progressive

retinal degeneration. Adv. Experiment. Med. Biol. 854, 31–37.

Brown, D.M., Campochiaro, P.A., Singh, R.P., Li, Z., Gray, S., Saroj, N., Rundle, A.C.,

Rubio, R.G., Murahashi, W.Y., 2010. Ranibizumab for macular edema following

central retinal vein occlusion: six-month primary end point results of a phase III

study. Ophthalmology 117, 1124–1133 e1121.

Brown, D.M., Heier, J.S., Clark, W.L., Boyer, D.S., Vitti, R., Berliner, A.J., Zeitz, O., Sandbrink,

R., Zhu, X., Haller, J.A., 2013. Intravitreal aflibercept injection for macular edema

secondary to central retinal vein occlusion: 1-year results from the phase 3

COPERNICUS study. Am. J. Ophthalmol. 155, 429–437 e427.

Brown, D.M., Kaiser, P.K., Michels, M., Soubrane, G., Heier, J.S., Kim, R.Y., Sy, J.P.,

Schneider, S., 2006. Ranibizumab versus verteporfin for neovascular age-related

macular degeneration. N. Engl. J. Med. 355, 1432–1444.

Burke, J.M., 2008. Epithelial phenotype and the RPE: is the answer blowing in the Wnt?

Prog. Retin. Eye Res. 27, 579–595.

Campbell, M., Doyle, S.L., Ozaki, E., Kenna, P.F., Kiang, A.S., Humphries, M.M., Humphries,

P., 2014. An overview of the involvement of interleukin-18 in degenerative

retinopathies. Adv. Experiment. Med. Biol. 801, 409–415.

Campochiaro, P.A., Heier, J.S., Feiner, L., Gray, S., Saroj, N., Rundle, A.C., Murahashi,

W.Y., Rubio, R.G., 2010. Ranibizumab for macular edema following branch retinal vein occlusion: six-month primary end point results of a phase III study. Ophthalmology 117, 1102–1112 e1101.

Chhablani, J., 2015. Intravitreal ziv-aflibercept for recurrent macular edema secondary to central retinal venous occlusion. Indian J. Ophthalmol. 63, 469–470.

Chhablani, J., Dedhia, C.J., Peguda, H.K., Stewart, M., 2017. SHORT-TERM safety OF 2 MG intravitreal ziv-aflibercept. Retina 37, 1859–1865.

Constable, P.A., Lawrenson, J.G., 2009. Glial cell factors and the outer blood retinal barrier. Ophthalmic Physiol. Opt. 29, 557–564.

de Oliveira Dias, J., Xavier, C., Maia, A., de Moraes, N., Meyer, C., Farah, M., Rodrigues, E., 2015. Intravitreal injection of ziv-aflibercept in patient with refractory age-related macular degeneration. Ophthalmic Surg Lasers Imaging Retina 46, 91–94.

de Oliveira Dias, J.R., Costa de Andrade, G., Kniggendorf, V.F., Novais, E.A., Takahashi, V.K.L., Maia, A., Meyer, C., Watanabe, S.E.S., Farah, M.E., Rodrigues, E.B., 2017. Intravitreal ziv-aflibercept for neovascular age-related macular degeneration: 52-week results. Retina Publish Ahead of Print.

de Oliveira Dias, J.R., de Andrade, G.C., Novais, E.A., Farah, M.E., Rodrigues, E.B., 2016. Fusion proteins for treatment of retinal diseases: aflibercept, ziv-aflibercept, and conbercept. International journal of retina and vitreous 2 3-3.

Deissler, H.L., Deissler, H., Lang, G.E., 2012. Actions of bevacizumab and ranibizumab on microvascular retinal endothelial cells: similarities and differences. Br. J. Ophthalmol. 96, 1023–1028.

Do, D.V., Nguyen, Q.D., Boyer, D., Schmidt-Erfurth, U., Brown, D.M., Vitti, R., Berliner,

A.J., Gao, B., Zeitz, O., Ruckert, R., Schmelter, T., Sandbrink, R., Heier, J.S., 2012. One-year outcomes of the DA VINCI study of VEGF trap-eye in eyes with diabetic macular edema. Ophthalmology 119, 1658–1665.

Do, D.V., Nguyen, Q.D., Khwaja, A.A., Channa, R., Sepah, Y.J., Sophie, R., Hafiz, G., Campochiaro, P.A., READ-2 Study Group, f.t., 2013. Ranibizumab for edema of the macula in diabetes study: 3-year outcomes and the need for prolonged frequent TreatmentRanibizumab for edema of the macula. JAMA Ophthalmology 131, 139–145.

Dunn, K.C., Aotaki-Keen, A.E., Putkey, F.R., Hjelmeland, L.M., 1996. ARPE-19, A human retinal pigment epithelial cell line with differentiated properties. Exp. Eye Res. 62, 155–170.

Franceschi, C., Campisi, J., 2014. Chronic inflammation (inflammaging) and its potential contribution to age-associated diseases. J. Gerontol. Ser. A Biol. Med. Sci. 69 (Suppl. 1), S4–S9.

Franze, K., Grosche, J., Skatchkov, S.N., Schinkinger, S., Foja, C., Schild, D., Uckermann, O., Travis, K., Reichenbach, A., Guck, J., 2007. Müller cells are living optical fibers in the vertebrate retina. Proc. Natl. Acad. Sci. 104, 8287–8292.

García, M., Vecino, E., 2003. Role of Müller glia in neuroprotection and regeneration in the retina. Histol. Histopathol. 18, 1205–1218.

Glisic-Milosavljevic, S., Waukau, J., Jana, S., Jailwala, P., Rovensky, J., Ghosh, S., 2005. Comparison of apoptosis and mortality measurements in peripheral blood mononuclear cells (PBMCs) using multiple methods. Cell Prolif 38, 301–311.

Golan, S., Entin-Meer, M., Semo, Y., Maysel-Auslender, S., Mezad-Koursh, D., Keren, G.,

Loewenstein, A., Barak, A., 2014. Gene profiling of human VEGF signaling pathways in human endothelial and retinal pigment epithelial cells after anti VEGF treatment. BMC Res. Notes 7, 617.

Goldberg, E.L., Dixit, V.D., 2015. Drivers of age-related inflammation and strategies for healthspan extension. Immunol. Rev. 265, 63–74.

Group, B.P.N.W., 2012. LA. C. Memorandum Addendum - BLA 125418 - Zaltrap ([xxx]-Aflibercept) Manufactured by Sanofi Aventis. U.S, LLC.

Grunwald, J.E., Daniel, E., Huang, J., Ying, G.-s., Maguire, M.G., Toth, C.A., Jaffe, G.J., Fine, S.L., Blodi, B., Klein, M.L., Martin, A.A., Hagstrom, S.A., Martin, D.F., 2014. Risk of geographic atrophy in the comparison of age-related macular degeneration treatments trials. Ophthalmology 121, 150–161.

Guo, B., Wang, Y., Hui, Y., Yang, X., Fan, Q., 2010. Effects of anti-VEGF agents on rat retinal Müller glial cells. Mol. Vis. 16, 793–799.

Hollborn, M., Ulbricht, E., Rillich, K., Dukic-Stefanovic, S., Wurm, A., Wagner, L., Reichenbach, A., Wiedemann, P., Limb, G.A., Bringmann, A., Kohen, L., 2011. The human Muller cell line MIO-M1 expresses opsins. Mol. Vis. 17, 2738–2750.

Idziorek, T., Estaquier, J., De Bels, F., Ameisen, J.-C., 1995. YOPRO-1 permits cytofluorometric analysis of programmed cell death (apoptosis) without interfering with cell viability. J. Immunol. Methods 185, 249–258.

Klettner, A., Möhle, F., Roider, J., 2010. Intracellular bevacizumab reduces phagocytotic uptake in RPE cells. Graefe's Arch. Clin. Exp. Ophthalmol. 248, 819–824.

Limb, G.A., Salt, T.E., Munro, P.M.G., Moss, S.E., Khaw, P.T., 2002. In vitro characterization of a spontaneously immortalized human Müller cell line (MIO-M1). Investig. Ophthalmol. Vis. Sci. 43, 864–869.

Luthra, S., Narayanan, R., Marques, L.E., Chwa, M., Kim, D.W., Dong, J., Seigel, G.M., Neekhra, A., Gramajo, A.L., Brown, D.J., Kenney, M.C., Kuppermann, B.D., 2006. Evaluation of in vitro effects of bevacizumab (Avastin) on retinal pigment epithelial, neurosensory retinal, and microvascular endothelial cells. Retina 26, 512–518.

Malik, D., del Carpio, J.C., Kim, Y.G., Moustafa, M.T.M., Thaker, K., Patel, T., Bababeygy, S.R., Kenney, C.M., Kuppermann, B., 2014a. Mitochondrial membrane potential response of retinal pigment epithelium cells in vitro to anti-VEGF agents: ranibizumab, bevacizumab, aflibercept and ziv-aflibercept. Investig. Ophthalmol. Vis. Sci. 55 599-599.

Malik, D., Tarek, M., Caceres del Carpio, J., Ramirez, C., Boyer, D., Kenney, M.C., Kuppermann, B.D., 2014b. Safety profiles of anti-VEGF drugs: bevacizumab, ranibizumab, aflibercept and ziv-aflibercept on human retinal pigment epithelium cells in culture. Br. J. Ophthalmol. 98, i11–i16.

Manousaridis, K., Talks, J., 2012. Macular ischaemia: a contraindication for anti-VEGF treatment in retinal vascular disease? Br. J. Ophthalmol. 96, 179–184.

Mansour, A.M., Al-Ghadban, S.I., Yunis, M.H., El-Sabban, M.E., 2015. Ziv-aflibercept in macular disease. Br. J. Ophthalmol. 99, 1055–1059.

Mansour, A.M., Ashraf, M., Dedhia, C.J., Charbaji, A., Souka, A.A.R., Chhablani, J., 2017a. Long-term safety and efficacy of ziv-aflibercept in retinal diseases. Br. J. Ophthalmol. 101, 1374–1376.

Mansour, A.M., Dedhia, C., Chhablani, J., 2017b. Three-month outcome of intravitreal

ziv-aflibercept in eyes with diabetic macular oedema. Br. J. Ophthalmol. 101,

166–169.

Martin, D.F., Maguire, M.G., Fine, S.L., Ying, G.-s., Jaffe, G.J., Grunwald, J.E., Toth, C.,

Redford, M., Ferris, F.L., 2012. Ranibizumab and bevacizumab for treatment of

neovascular age-related macular degeneration: two-year results. Ophthalmology 119,

1388–1398.

Matsuda, M., Krempel, P.G., Marquezini, M.V., Sholl-Franco, A., Lameu, A., Monteiro,

M.L.R., Miguel, N.C.d.O., 2017. Cellular stress response in human Müller cells

(MIOM1) after bevacizumab treatment. Exp. Eye Res. 160, 1–10.

Matsuzaki, K., Tomioka, M., Watabe, Y., 2014. Expression of the sortilin gene in cultured

human keratinocytes increases in a glucose-free medium. Clin Res Foot Ankle 1–5.

Mosmann, T., 1983. Rapid colorimetric assay for cellular growth and survival: application

to proliferation and cytotoxicity assays. J. Immunol. Methods 65, 55–63.

Ozawa, Y., Toda, E., Kawashima, H., Homma, K., Osada, H., Nagai, N., Abe, Y., Yasui, M.,

Tsubota, K., 2019. Aquaporin 4 suppresses neural hyperactivity and synaptic fatigue

and fine-tunes neurotransmission to regulate visual function in the mouse retina.

Mol. Neurobiol. 12 019-01661.

Pereiro, X., Ruzafa, N., Acera, A., Fonollosa, A., Rodriguez, F.D., Vecino, E., 2018.

Dexamethasone protects retinal ganglion cells but not Muller glia against

hyperglycemia in vitro. PLoS One 13.

Ramírez, C., Cáceres-del-Carpio, J., Chu, J., Chu, J., Moustafa, M.T., Chwa, M., Limb,

G.A., Kuppermann, B.D., Kenney, M.C., 2016. Brimonidine can prevent in vitro hydroquinone

    damage on retinal pigment epithelium cells and retinal Müller cells. J. Ocul.

    Pharmacol. Ther. 32, 102–108.

Reichenbach, A., Bringmann, A., 2013. New functions of Müller cells. Glia 61, 651–678.

Rios, M.N., Marchese, N.A., Guido, M.E., 2019. Expression of non-visual opsins Opn3 and

    Opn5 in the developing inner retinal cells of birds. Light-responses in muller glial

    cells. Front. Cell. Neurosci. 13.

Romano, M.R., Biagioni, F., Besozzi, G., Carrizzo, A., Vecchione, C., Fornai, F., Lograno,

    M.D., 2012. Effects of bevacizumab on neuronal viability of retinal ganglion cells in

    rats. Brain Res. 1478, 55–63.

Rosenfeld, P.J., Brown, D.M., Heier, J.S., Boyer, D.S., Kaiser, P.K., Chung, C.Y., Kim, R.Y.,

    2006. Ranibizumab for neovascular age-related macular degeneration. N. Engl. J.

    Med. 355, 1419–1431.

Sarthy, P., Lam, D., 1978. Biochemical studies of isolated glial (muller) cells from the

    turtle retina. J. Cell Biol. 78, 675–684.

Schnichels, S., Hagemann, U., Januschowski, K., Hofmann, J., Bartz-Schmidt, K.-U.,

    Szurman, P., Spitzer, M.S., Aisenbrey, S., 2013. Comparative toxicity and proliferation

    testing of aflibercept, bevacizumab and ranibizumab on different ocular cells. Br.

    J. Ophthalmol. 97, 917–923.

Singh, S.R., Dogra, A., Stewart, M., Das, T., Chhablani, J., 2017. Intravitreal ziv-aflibercept:

    clinical effects and economic impact. Asia Pac J Ophthalmol 6, 561–568.

Spitzer, M.S., Yoeruek, E., Sierra, A., Wallenfels-Thilo, B., Schraermeyer, U., Spitzer, B.,

    Bartz-Schmidt, K.U., Szurman, P., 2007. Comparative antiproliferative and cytotoxic

    profile of bevacizumab (Avastin), pegaptanib (Macugen) and ranibizumab (Lucentis)

on different ocular cells. Graefe's Arch. Clin. Exp. Ophthalmol. 245, 1837–1842.

TDRCR, N., 2015. Aflibercept, bevacizumab, or ranibizumab for diabetic macular edema. N. Engl. J. Med. 372, 1193–1203.

Tian, J., Ishibashi, K., Honda, S., Boylan, S.A., Hjelmeland, L.M., Handa, J.T., 2005. The expression of native and cultured human retinal pigment epithelial cells grown in different culture conditions. Br. J. Ophthalmol. 89, 1510–1517.

Tufail, A., Patel, P.J., Egan, C., Hykin, P., da Cruz, L., Gregor, Z., Dowler, J., Majid, M.A., Bailey, C., Mohamed, Q., Johnston, R., Bunce, C., Xing, W., 2010. Bevacizumab for neovascular age related macular degeneration (ABC Trial): multicentre randomised double masked study. BMJ 340, c2459.

Wu, P.C., Chen, Y.J., Chen, C.H., Chen, Y.H., Shin, S.J., Yang, H.J., Kuo, H.K., 2008. Assessment of macular retinal thickness and volume in normal eyes and highly myopic eyes with third-generation optical coherence tomography. Eye 22, 551–555.

Zehetner, C., Bechrakis, N.E., Stattin, M., Kirchmair, R., Ulmer, H., Kralinger, M.T., Kieselbach, G.F., 2015. Systemic counterregulatory response of placental growth factor levels to intravitreal aflibercept TherapySystemic PlGF upregulation after intravitreal aflibercept. Investig. Ophthalmol. Vis. Sci. 56, 3279–3286.
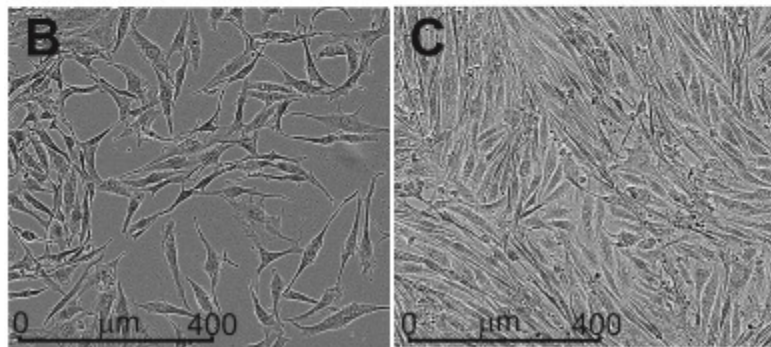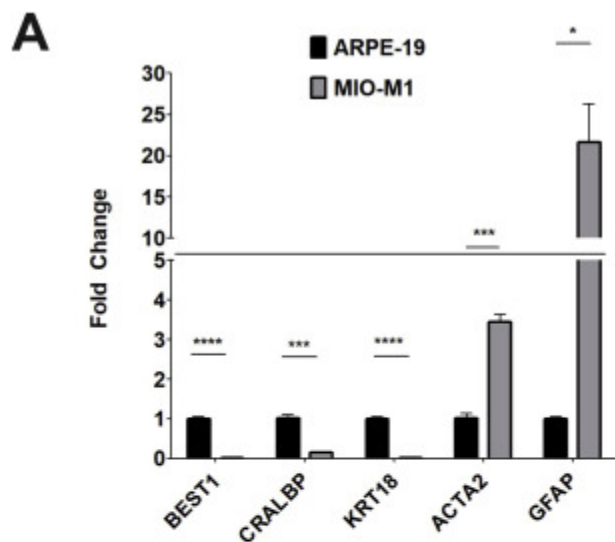
Fig. 1. (**A**) Gene expression levels for Müller cell markers to validate the MIO-M1 cell line. The MIO-M1 and ARPE-19 cells were analyzed by qRT-PCR. ARPE-19 samples were assigned a value of 1 for each of the markers. Genes expression levels of the *ACTA2* ($p = 0.0003$) and the *GFAP* ($p = 0.01$) were significantly higher in MIO-M1 cells compared to ARPE-19 cells. MIO-M1 cells had very low levels for the three known ARPE-19 markers (*BEST1,* $p = 0.0.0001$; *CRALBP*, $p = 0.0007$; and *KRT18,* $p = 0.0001$). (**B**) Subconfluent monolayer of MIO-M1 cells shows bipolar extensions, elongated cytoplasmic projections and a granular intracellular profile. (**C**) Confluent monolayer of MIO-M1 cells shows MIO-M1 cells maintain their spindle shape and granular appearance.
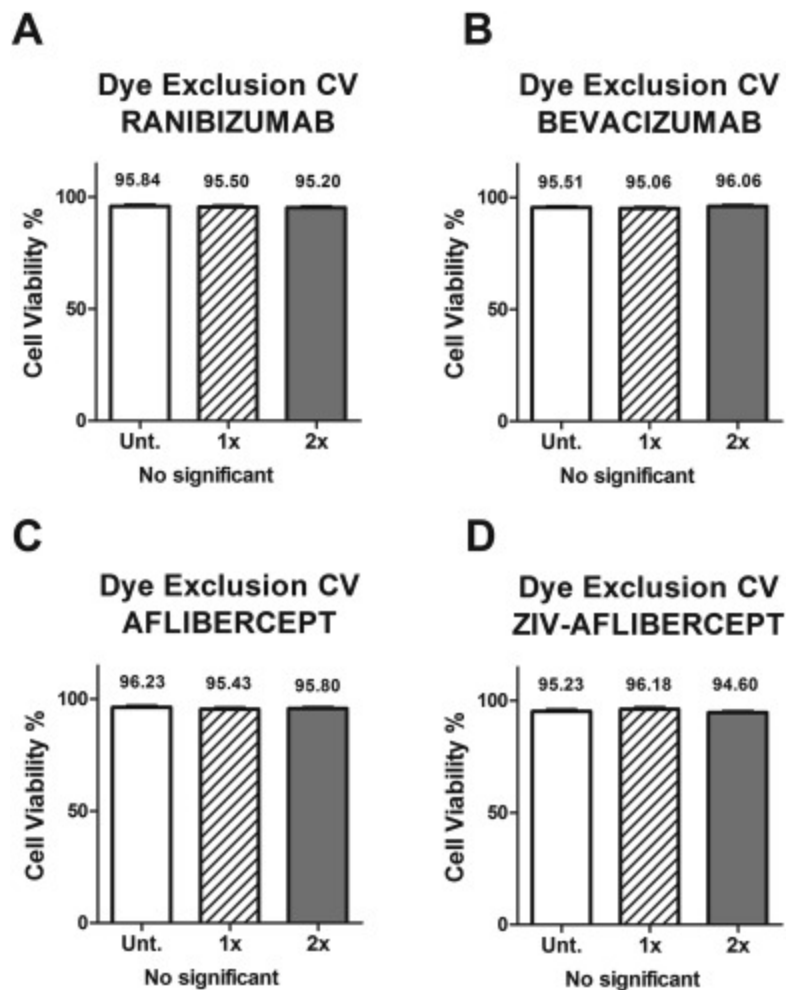
Fig. 2. Cell viability (CV) percentage differences measured by the Trypan blue dye exclusion assay shows no differences between untreated and the tested anti-VEGF treated MIO-M1 cell cultures in the 2 dosage concentrations. Each group (untreated, 1x and 2x) was plated in duplicate and repeated 3 times. All p values were greater than 0.05 showing non-statistical significance. 1x: equivalent to the clinical doses of anti-VEGF (0.05 ml injected in 4 ml of vitreous). 2x: equivalent to double the clinical dose of anti-VEGF.
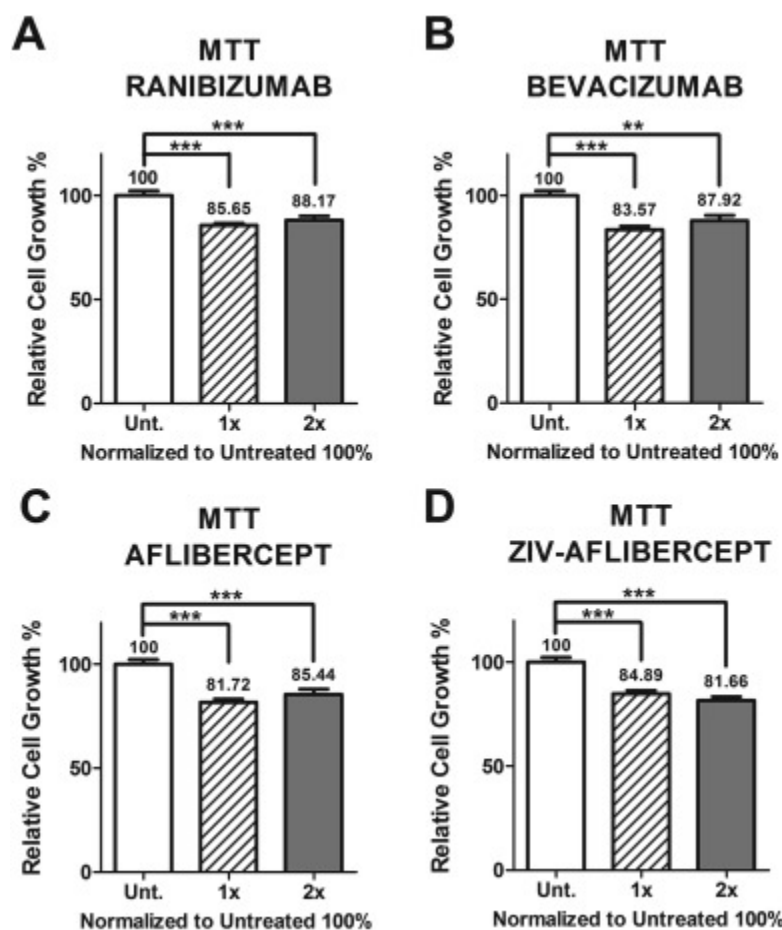
Fig. 3. Cellular metabolic activity was measured by the MTT assay and shows the relative cell growth percentage differences between untreated and anti-VEGF treated MIO-M1 cells with the different concentration dosages. Each group (untreated, 1x and 2x) was plated in duplicate and repeated 3 times. *: p value < 0.05; **: p value < 0.01; ***: p value < 0.001; values with non-statistical significance (p > 0.05) have no * signaling. Control samples assigned a value of 100%. 1x: equivalent to the clinical doses of anti-VEGF (0.05 ml injected in 4 ml of vitreous). 2x: equivalent to double the clinical dose of anti-VEGF.
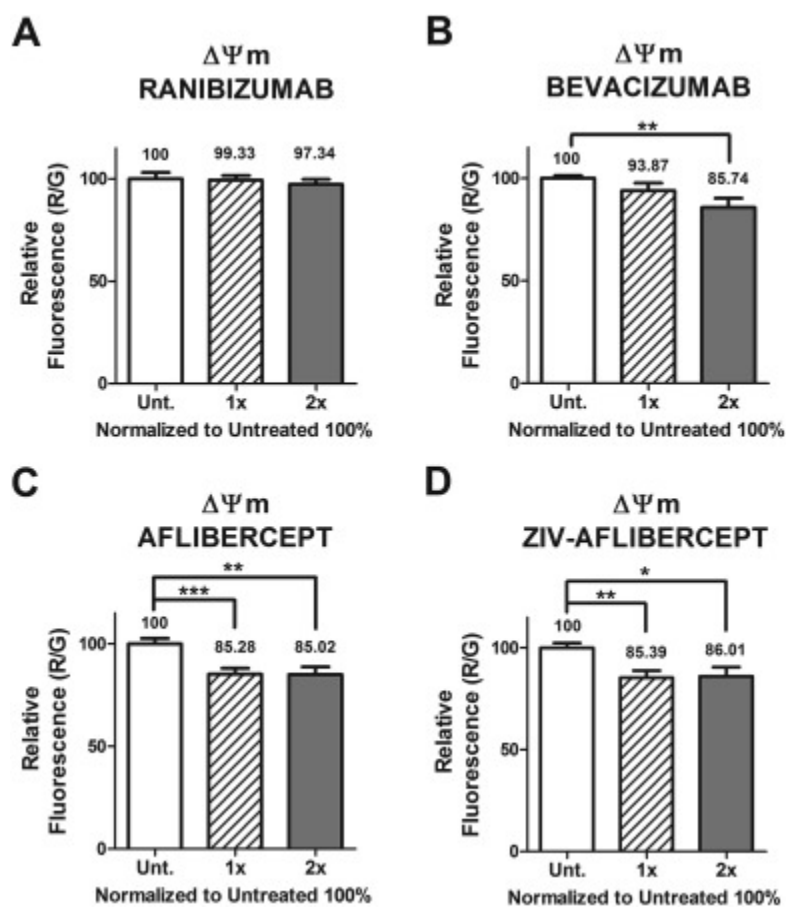
Fig. 4. The mitochondrial membrane potential (ΔΨm) assay shows a decrease in relative fluorescence anti-VEGF treated MIO-M1 cells compared to untreated cultures, in all except with 1 anti-VEGF treatment. Each group (untreated, 1x and 2x) was plated in duplicate and repeated 3 times. *: p value < 0.05; **: p value < 0.01; ***: p value < 0.001; values with non-statistical significance (p > 0.05) have no * signaling. Control samples assigned a value of 100%. 1x: equivalent to the clinical doses of anti-VEGF (0.05 ml injected in 4 ml of vitreous). 2x: equivalent to double the clinical dose of anti-VEGF.
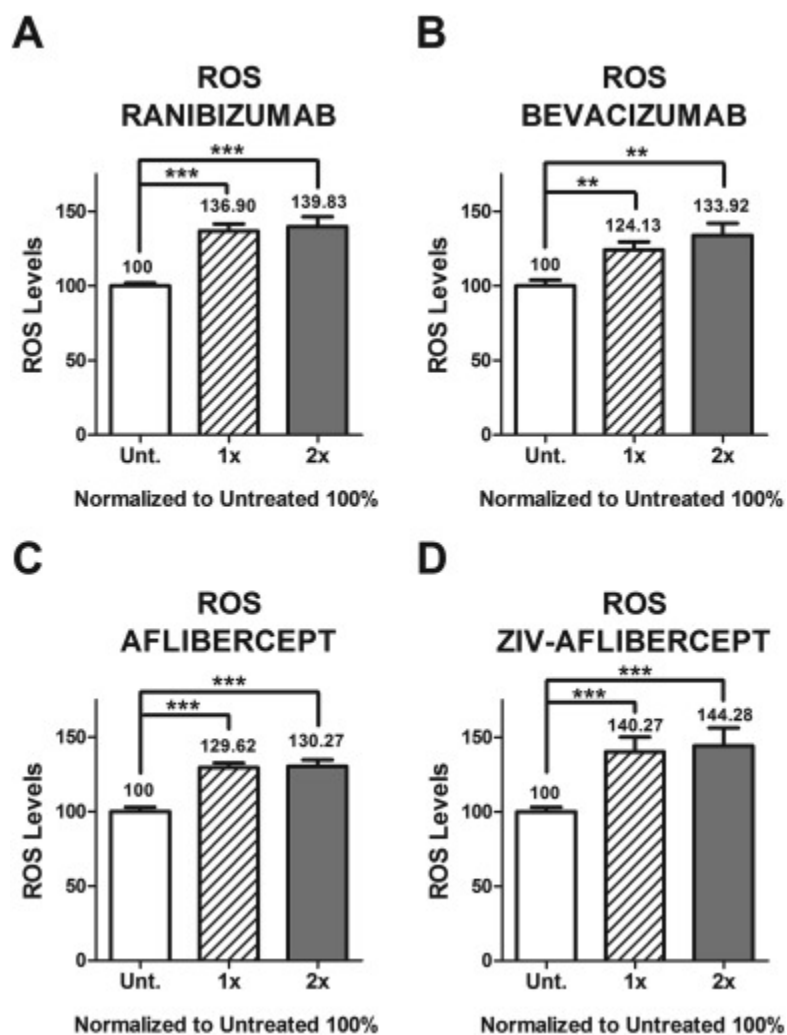
Fig. 5. The levels of ROS production increased in anti-VEGF treated MIO-M1 cells compared to untreated cultures, with the different concentration dosages. Each group (untreated, 1x and 2x) was plated in duplicate and repeated 3 times. *: p value < 0.05; **: p value < 0.01; ***: p value < 0.001; values with non-statistical significance (p > 0.05) have no * signaling. Control samples assigned a value of 100%. 1x: equivalent to the clinical doses of anti-VEGF (0.05 ml injected in 4 ml of vitreous). 2x: equivalent to double the clinical dose of anti-VEGF.
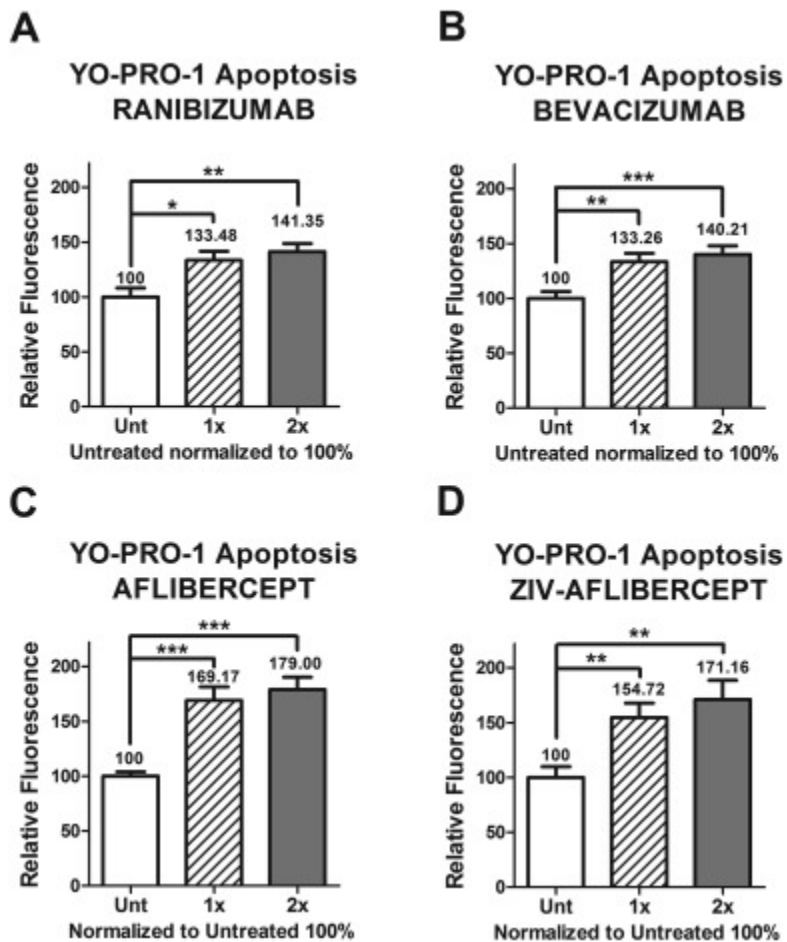
Fig. 6. The YO-PRO-1 apoptosis assay shows increased relative fluorescence levels in the anti-VEGF treated MIO-M1 cells compared to untreated, with the different concentration dosages. Each group (untreated, 1x and 2x) was plated in duplicate and repeated 3 times. *: p value < 0.05; **: p value < 0.01; ***: p value < 0.001; values with non-statistical significance (p > 0.05) have no * signaling. Control samples assigned a value of 100%. 1x: equivalent to the clinical doses of anti-VEGF (0.05 ml injected in 4 ml of vitreous). 2x: equivalent to double the clinical dose of anti-VEGF.

Cáceres-del-Carpio Table 1. Gene symbol, name, gene bank accession number and function.

Gene Symbol[a]	Gene Name[b]	Gene Bank Accession Num.[c]	Function[d]
GPX3	Glutathione peroxidase 3	NM_002084	Catalyzes the reduction of hydrogen peroxide.
SOD2	Superoxide dismutase 2, mitochondria	NM_000636, NM_001024465	Converts the superoxide byproducts to H_2O_2 and O_2.
IL1β	Interleukin 1, beta (also known as IL-1β)	NM_000576, XM_006712496	Encodes a cytokine involving cell proliferation, differentiation and apoptosis.
IL18	Interleukin 18	NM_001243211, NM_001562	Cytokine that stimulates natural killer cell activity and interferon gamma production.
BCL2L13	BCL2-like 13 (apoptosis facilitator)	NM_015367	Encodes a mitochondrial-localized protein. Overexpression results in apoptosis.
BAX	BCL2-associated X protein (also known as BCL2L4)	NM_004324, NM_138761, NM_138763, NM_138764, NM_138765, NR_027882, NM_001291428, NM_001291429, NM_001291430, NM_001291431, XM_006723314	Encodes a pro-apoptotic protein.
VEGFA	Vascular endothelial growth factor A	NM_001025366, NM_001025367, NM_001025368, NM_001033756, NM_001171623, NM_001171624, NM_001171625, NM_001171626, NM_001171629, NM_003376, NM_001287044	Encodes a protein that induces angiogenesis, vasculogenesis and inhibition of apoptosis.
PGF	Placental growth factor (also known as PLGF)	NM_001207012, NM_002632, NM_001293643	Encodes a growth factor homologous to vascular endothelial growth factor.

Gene Symbol[a]	Gene Name[b]	Gene Bank Accession Num.[c]	Function[d]
HIF1A	Hypoxia inducible factor 1 alpha	NM_001243084, NM_001530, NM_181054	In response to adaptation to hypoxia, activates transcription of genes involved in energy metabolism, angiogenesis, apoptosis and oxygen delivery.

a. Official gene symbol by HUGO (Human Genome Organization) Gene Nomenclature Committee (HGNC);

b. Official gene name by HUGO Gene Nomenclature Committee (HGNC).

c. Gene Accession Bank Number from the primers used (Qiagen, Valencia, CA).

d. Gene function modified from PubMed gene.

Table 2. Differences in gene expression of MIO-M1 cells after treatment with 1x and 2x anti-VEGF drugs 2A. Treated with Ranibizumab. 2B Treated with bevacizumab. 2C Treated with aflibercept. 2D Treated with ziv-aflibercept.

Table 2A. MIO – M1 treated with ranibizumab

	1x		2x	
Gene	Fold	P	Fold	p
VEGFA[†]	0.66	0.029*	0.41	0.0008*
PGF[†]	1.11	0.55	1.41	0.066
HIF1A[†]	1.2	0.29	2.26	0.094
BAX[‡]	1.06	0.58	0.93	0.56
BCL2L13[‡]	0.91	0.23	1.05	0.55
IL1β[§]	5.12	0.0001*	4.58	0.0002*
IL18[§]	1.43	0.0175*	1.39	0.017*
GPX3[#]	2.31	0.0001*	1.96	0.0001*
SOD2[#]	0.58	0.002*	0.3	0.0006*

Table 2B. MIO-M1 treated with bevacizumab

	1x		2x	
Gene	Fold	p	Fold	p
VEGFA[†]	0.65	0.0016*	0.41	0.0187*
PGF[†]	1.79	0.0132*	1.49	0.036
HIF1A[†]	1.41	0.35	0.94	0.92
BAX[‡]	1.22	0.0114*	1.01	0.82
BCL2L13[‡]	1.38	0.0015*	1.6	0.0007*
IL1β[§]	1.8	0.0041*	1.19	0.15
IL18[§]	1.57	0.13	1.1	0.73
GPX3[#]	2.13	0.0011*	2.22	0.0006*
SOD2[#]	0.69	0.0402*	0.41	0.0013*

Table 2C. MIO-M1 treated with aflibercept

	1x		2x	
Gene	Fold	p	Fold	P
VEGFA[†]	0.55	0.0037*	0.58	0.0136*
PGF[†]	2.2	0.0147*	1.84	0.0108*
HIF1A[†]	1.48	0.22	1.34	0.26
BAX[‡]	0.98	0.75	1.08	0.19
BCL2L13[‡]	1.35	0.0094*	1.21	0.0132*

	1x		2x	
IL1β§	1.19	0.2	0.89	0.6
IL18§	0.63	0.19	0.95	0.85
GPX3#	2.18	0.0002*	1.67	0.001*
SOD2#	0.22	<0.0001*	0.44	0.0014*

Table 2D. MIO-M1 treated with ziv-Aflibercept

	1x		2x	
Gene	Fold	p	Fold	p
VEGFA†	0.88	0.014*	0.92	0.618
PGF†	0.7	0.0245*	0.53	0.0063*
HIF1A†	1.06	0.69	1.09	0.61
BAX‡	1.85	0.0009*	1.46	0.0005*
BCL2L13‡	1.04	0.485	1.29	0.053
IL1β§	1	0.99	1.21	0.563
IL18§	1.96	0.0164*	1.88	0.0168*
GPX3#	0.95	0.457	1.17	0.156
SOD2#	0.22	<0.0001*	0.24	<0.0001*

9 genes were tested, each one was tested 2 times in triplicate.

Fold values > 1 indicates upregulation of the gene compared with untreated control; Fold values < 1 indicates downregulation of the gene compared with untreated control; Control samples assigned a value of 1.

1x: equivalent to the clinical doses of anti-VEGF (0.05 ml injected in 4 ml of vitreous).

2x: equivalent to double the clinical dose of anti-VEGF.

Folds were calculated with the formula 2ΔΔCt.*p < 0.05; † Angiogenesis; ‡ Pro-apoptosis; § Inflammation; # Oxidative stress.